Ming Zhu*, Hongfang Ma, Mingjing Wang, Zhihua Wang and Adel Sharif*

Effects of Cations on Corrosion of Inconel 625 in Molten Chloride Salts

Abstract: Hot corrosion of Inconel 625 in sodium chloride, potassium chloride, magnesium chloride, calcium chloride and their mixtures with different compositions is conducted at 900 °C to investigate the effects of cations in chloride salts on corrosion behavior of the alloy. XRD, SEM/EDS were used to analyze the compositions, phases, and morphologies of the corrosion products. The results showed that Inconel 625 suffers more severe corrosion in alkaline earth metal chloride molten salts than alkaline metal chloride molten salts. For corrosion in mixture salts, the corrosion rate increased with increasing alkaline earth metal chloride salt content in the mixture. Cations in the chloride molten salts mainly affect the thermal and chemical properties of the salts such as vapor pressure and hydroscopicities, which can affect the basicity of the molten salt. Corrosion of Inconel 625 in alkaline earth metal chloride salts is accelerated with increasing basicity.

Keywords: corrosion, molten salts, chlorides, cation, Inconel alloy

DOI 10.1515/htmp-2014-0225
Received December 2, 2014; accepted March 10, 2015

Introduction

High-temperature corrosion of metallic boiler tubes by alkali chlorides is the primary limiting factor for efficiency of waste and biofuel power generators [1–5]. Development of protection techniques for improving durability and safety of metal alloy components for high-temperature environments containing chlorides requires thorough understanding of the corrosion mechanisms involved. Limited data are available on corrosion in molten chlorides compared with molten sulfates and carbonates. The mechanisms of accelerated corrosion caused by chloride salts are not fully understood.

Several mechanisms have been proposed to explain the rapid high-temperature corrosion of metals in chloride-ion-containing environments. The most widely accepted theory is the so-called active oxidation mechanism [5]. Reaction of molecular chlorine with metals results in the formation of alkali chlorides. Reaction of these chlorides with oxygen at the sample surface results in the formation and growth of a porous oxide layer. This reaction frees chlorine to reenter the oxidation cycle and react with cations in the bulk material. The metal chloride formed is stable due to low partial pressure of oxygen at the oxide/metal interface. However, as it penetrates through cracks and pores in the oxide scale, it accesses oxygen, undergoes oxidation, deposits a molecule of metal oxide at the scale and releases chlorine. As the oxide scale grows, oxidation rate is controlled by inward diffusion of chlorine to the oxide/metal interfaces and outward penetration of volatile metal chloride. Chlorine is the "active oxidation" agent as it diffuses in and out of the oxide scale without being consumed.

This cycle requires low oxygen partial pressure at the metal/oxide scale interface and the transport of molecular chlorine and transition-metal chloride gas through the oxide scale. Lehmusto et al. pointed out that it is unexpected that the molecular chlorine and transition-metal chlorides with larger radii can penetrate the oxide scale while the molecular oxygen with smaller radius cannot [6]. It has been suggested that the formation of alkali chromates, which has been substantiated by XRD analysis, destroys integrity of the protective chromium oxide scale and allows penetration, rather than diffusion, of molecular chlorine through cracks in the oxide scale [7]. Investigations on corrosion behavior of chromium powder with eight different chloride salts at temperature range of 400–600°C indicated that $BaCl_2$, $CaCl_2$ and $MgCl_2$ do not react with chromium at these temperatures, KCl, LiCl, NaCl, and $PbCl_2$ are reactive and can accelerate

***Corresponding author: Ming Zhu,** College of Materials Science and Engineering, Xi'an University of Science and Technology, Xi'an 710054, China, E-mail: mingzhu@xust.edu.cn
Adel Sharif, Department of Mechanical Engineering, California State University, Los Angeles, CA 90032, USA,
E-mail: aasharif@exchange.calstatela.edu
Hongfang Ma, Mingjing Wang, Zhihua Wang, College of Materials Science and Engineering, Xi'an University of Science and Technology, Xi'an 710054, China

the oxidation of chromium above 500°C, whereas $ZnCl_2$ evaporates [6]. Enestam et al. discovered some differences in the corrosive effects of NaCl and KCl salts on degradation of two austenitic stainless steels and one low alloy steel under experimental conditions considered [8].

In general, chloride-induced corrosion investigations are carried out in biomass and waste-derived fuel combustion environments [9–11]. The chloride salts are deposited on the sample surface as thin films at high-temperature gaseous corrosive environments. It is important to note that in solar thermal plants and nuclear reactors, the alloy components are immersed in the molten chloride salts. Investigations conducted in the gaseous environments are not representative of the highly corrosive aqueous environments of solar thermal plants and nuclear reactors.

The present study investigates the role of cations in inducing corrosion by chloride molten salts in boiler tubes. Herein, a comparative study of the hot corrosion of a Ni-based alloy (Inconel 625) in sodium chloride, potassium chloride, magnesium chloride, calcium chloride and their mixtures with different compositions at 900°C is conducted to understand the effects of cations in the chloride salt on the corrosion behavior Ni-based alloys. As a potential working mass for energy storage in solar plants, chloride salts may be utilized at temperatures around 900°C, whence the same temperature is chosen for the present investigations.

Experimental procedure

The chemical composition of Inconel 625 is listed in Table 1. In preparation for the corrosion tests, the as-received Inconel 625 sheet was cut into 10 mm × 10 mm × 4 mm samples by electro-discharge machining. The specimens were ground with 200, 600 and 1,000 grit SiC sand papers, polished by 0.3 μm alumina paste, rinsed with distilled water, ultrasonically degreased with acetone, and dried under a warm air stream.

Table 1: Main chemical composition of Inconel 625 alloy (mass %).

Elements	Ni	Cr	Mo	Nb + Ta	Fe
Content	61.2	22.25	9.65	3.75	3.15

Two alkali chloride salts, NaCl and KCl, and two alkaline earth chloride salts, $MgCl_2$ and $CaCl_2$, were chosen to study the effects of cations on corrosion of Inconel 625. In addition, corrosion tests were conducted in the mixtures of the four aforementioned chloride salts. All of the chloride salts were chemically pure to 99.99%. The as-received NaCl and KCl were anhydrous while $MgCl_2$ and $CaCl_2$ were hydrous. The composition of the mixture chloride salts is listed in Table 2. Each sample was buried in salts in a 50-cc alumina crucible individually, the ratio of the sample surface area to the weight of the chloride salt is about 360 mm^2/50 g. The corrosion tests were carried out in a Muffle furnace at 900°C. The crucibles were removed from the furnace every 5 h for the single chloride molten salt corrosion tests and every 2 h for the mixture chlorides molten salt corrosion tests. The samples were separated from molten salts immediately; they were cleansed of salt residue in boiling water for 20 min and dried in air prior to weight measurements by an analytical balance with 10^{-5} g sensitivity. After weight measurements, the samples were buried in fresh chloride salts to continue high-temperature corrosion tests. Corrosion tests in four different single chloride molten salts were repeated at 900°C because samples disintegrated during first trial in $MgCl_2$ and $CaCl_2$ molten salts after 20 h.

Table 2: Composition of the mixture chloride salts.

Sample	Salt mixture	Mass ratio
1	NaCl + $MgCl_2$	2:3
2	NaCl + $MgCl_2$	7:3
3	KCl + $MgCl_2$	2:3
4	KCl + $MgCl_2$	7:3
5	NaCl + $CaCl_2$	2:3
6	KCl + $CaCl_2$	2:3

Phase composition analysis of the corrosion products and the salts near the samples after corrosion tests were determined by x-ray diffraction (XRD, Rigaku D/max-2400, Japan) with Cu Kα. The XRD worked at 40 KV, the scanning range is 10°–80° and the scanning rate is 6.0 degree/min. Surface and cross-sections of the samples were analyzed by a scanning electron microscope (SEM, JSM-6390, JEOL, Japan) equipped with EDS.

Results

Corrosion kinetics

The plots of specific mass change vs corrosion time of Inconel 625 in four different chloride molten salts at 900°C are shown in Figure 1. Weight loss was observed in all

samples. A significant difference in corrosion rates was observed between samples corroded in alkali metal chloride and alkaline earth metal chloride molten salts while the rates were similar in each group. The dimensions of the samples corroded in NaCl and KCl did not change significantly in contrast to the large change in the size of the samples corroded in $CaCl_2$ and $MgCl_2$.

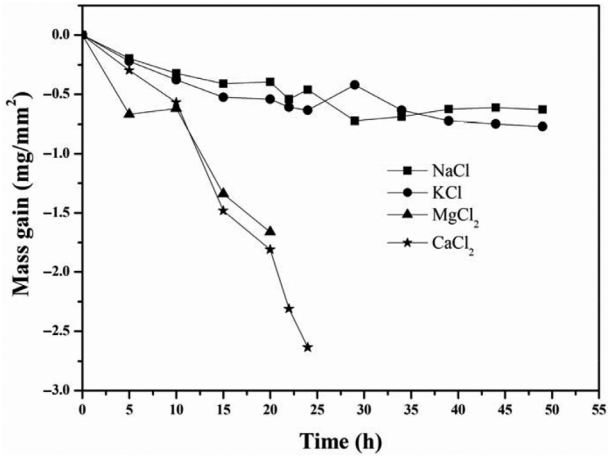

Figure 1: Corrosion kinetics of Inconel 625 in four molten chloride salts at 900°C.

Figure 2 is the compilation of the data for corrosion of Inconel 625 in six different mixtures of chlorides molten salts. Comparison to Figure 1 reveals that the corrosion rates of Inconel 625 in the mixtures are higher than those in the single alkali metal chloride molten salts but lower than those in the single alkaline earth metal chloride molten salts. Corrosion rates of Inconel 625 increased with increasing fraction of $MgCl_2$ in both NaCl and KCl salts. Corrosion rates of the samples in the mixtures containing KCl were higher than those containing NaCl for the same amount of either $MgCl_2$ or $CaCl_2$. However, a higher corrosion rate was observed for 40% KCl + 60% $MgCl_2$ mixture compared with 40% KCl + 60% $CaCl_2$ mixture.

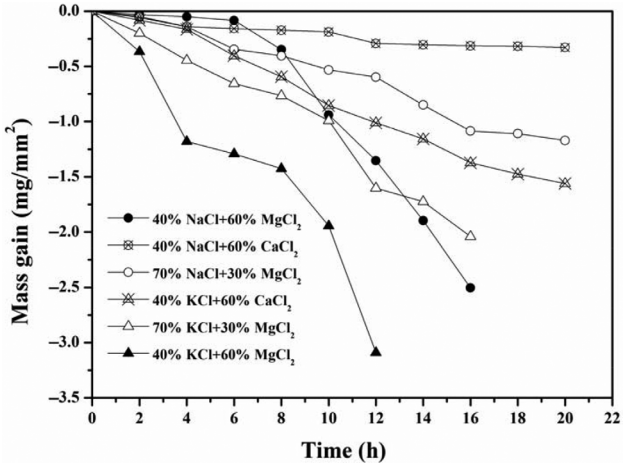

Figure 2: Corrosion kinetics of Inconel 625 in mixtures of molten chloride salts at 900°C.

XRD analysis of the corrosion products

Figure 3 shows the XRD patterns of the corrosion products formed on the surface of the samples in four different single chloride molten salts at 900°C. The corrosion products formed in the NaCl, KCl molten salts were mainly composed of Cr_2O_3 and $NiCr_2O_4$. The NaCl and KCl peaks observed were due to residual molten salts that were not washed away. Prior to performing XRD analysis, the top layer of the oxide scales of the samples corroded in $MgCl_2$ and $CaCl_2$ molten salts peeled off while being washed in hot water. XRD analysis was performed on the peeled scales. Determined from the intensities of their diffraction peaks, the oxide scale formed in $CaCl_2$ was $NiCr_2O_4$ for the most part with some Cr_2O_3. This reflects the composition of

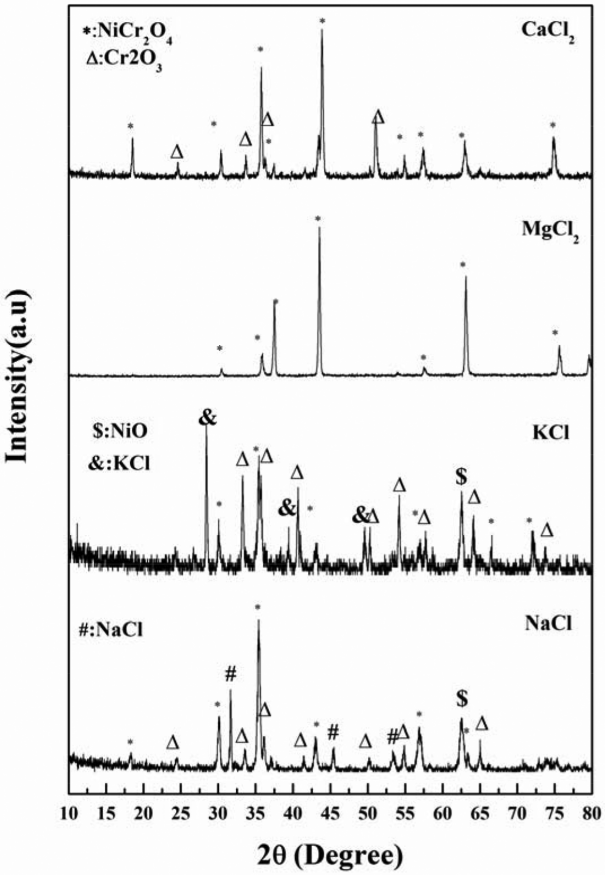

Figure 3: XRD patterns of the corrosion products formed on Inconel 625 in molten chloride salts at 900°C.

Inconel 625, which has 61.2 wt% Ni and 22.25 wt% Cr. Cr_2O_3 was not detected in the oxide scale of sample corroded in $MgCl_2$. It is possible that Cr_2O_3 remained undetected beneath other phases or was washed away with a layer of salt as indicated by the missing salt residue in x-ray diffraction data for sample tested in $CaCl_2$. In addition to $NiCr_2O_4$, another oxidation product, NiO, was observed on the sample tested in KCl. Diffraction results obtained for NaCl test are similar to those of $CaCl_2$ except for the residual salt remaining on the sample.

The XRD results of the scales that were peeled-off from the samples are listed in Table 3. There was not enough material for XRD analysis in the scales that peeled off in NaCl and KCl salts; therefore, they are missing in Table 3. It can be seen that the scale formed in $MgCl_2$ molten salt was mainly composed of $MgCr_2O_4$, $NiCr_2O_4$, and Cr_2O_3, whereas only $NiCr_2O_4$ formed in $CaCl_2$. Results of the XRD analysis on the salts near the samples after corrosion tests are also given in Table 3. The matter near the samples were still mainly the original salts after corrosion tests in NaCl and KCl molten salts, no other phase was detected; it is possible that the secondary phases were below the limit of detection of XRD. $MgCl_2$, $MgCr_2O_4$, $NiCrO_3$ and MgO and $CaCl_2$ CaO and $CaCl_2(H_2O)_2$ were detected in the salts adjacent to the sample after corrosion tests in $MgCl_2$ and $CaCl_2$ molten salts, respectively evincing highly corrosive effect of alkaline earth metal chloride molten salts on Inconel 625.

Table 3: Results of the XRD analysis on the salts near the samples after corrosion tests.

Molten salt	Phases detected in the salt near the sample	Phases detected in the peeled off oxides scales
NaCl	NaCl	–
KCl	KCl	–
$MgCl_2$	$MgCr_2O_4$, $NiCrO_3$, MgO_2	$MgCr_2O_4$, $NiCr_2O_4$, Cr_2O_3
$CaCl_2$	$CaCl_2$, CaO, $CaCl_2(H_2O)_2$	$NiCr_2O_4$, Cr_2O_3

X-ray diffraction patterns of the corrosion products formed in mixtures of chloride molten salts after corrosion at 900°C for 20 h are shown in Figure 4. It can be seen that only $NiCr_2O_4$ formed on the surfaces of the Inconel 625 during corrosion in $MgCl_2$ containing mixtures, while corrosion products formed in the $CaCl_2$ containing mixtures were composed of Cr_2O_3 and $NiCr_2O_4$.

Except for $MgCl_2$, no peaks corresponding to alkali or alkaline earth chromates were detected in the patterns of the corrosion products formed in the single chloride molten salts. However, the possibility of formation of alkali chromates cannot be eliminated since XRD can only detect phases with mass fractions above 5%.

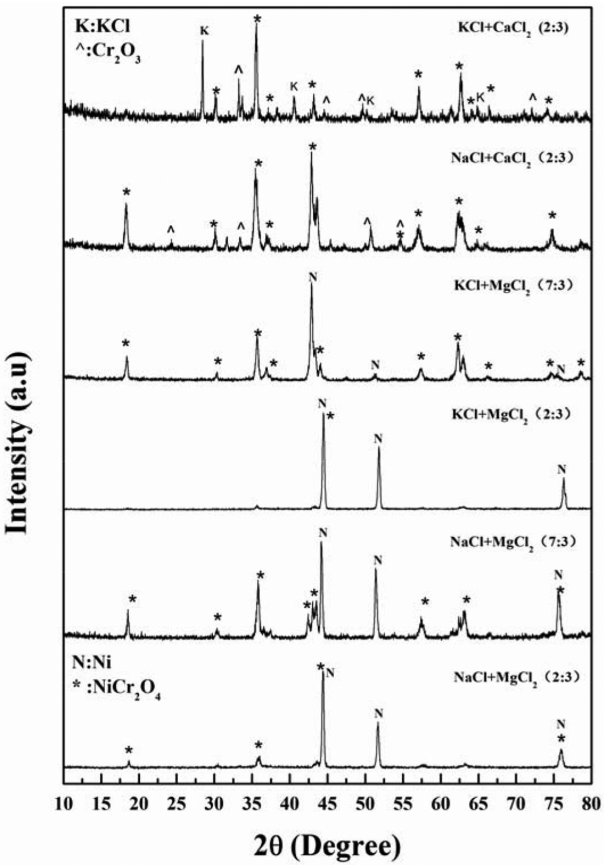

Figure 4: XRD patterns of the corrosion products formed during corrosion of Inconel 625 in mixtures of molten chloride salts at 900°C after 20 h.

Morphologies of the corrosion products

Surface morphologies

Surface morphologies of the corrosion products formed in four different single chloride molten salts after 20 h at 900°C are shown in Figure 5. As mentioned above, severe spallation of the corrosion products occurred in $MgCl_2$ and $CaCl_2$ molten salts during corrosion testing. Thus, Figure 5(c) and 5(d) depict the sample surface beneath the oxide scale. Comparison of the figures indicates that oxide layer is more porous than the layer beneath the scale, as expected. The grain size of the corrosion products depended on the corrosion rate of the molten salt. Also the grain size of the corrosion products formed in KCl molten salts is larger than that formed in NaCl molten salt and that of formed in $MgCl_2$ molten salt is larger than the one formed in $CaCl_2$ molten salt.

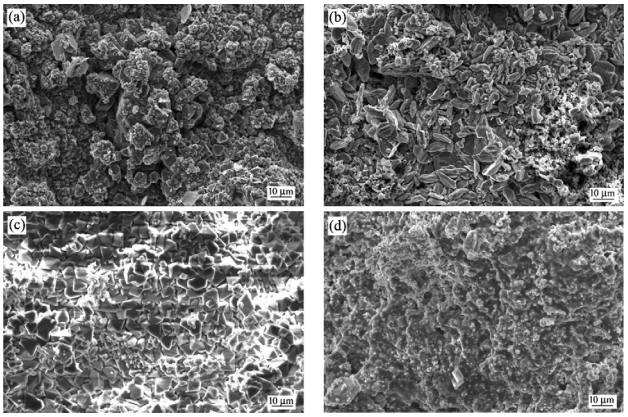

Figure 5: Surface morphology of Inconel 625 after corrosion in molten (a) NaCl, (b) KCl, (c) $MgCl_2$ and (d) $CaCl_2$ salts at 900°C.

Surface morphologies of the corrosion products formed in the mixture chloride molten salts after 20 h at 900°C are shown in Figure 6. All of the corrosion products are porous. The oxide scale formed in the most corrosive mixture, i. e. 40% KCl + 60% $MgCl_2$ mixture molten salt, is the most porous of all samples. Average hole size in the oxide scale was about 5 μm as seen in Figure 6(c). No holes were found in the oxide scale formed in 70% KCl + 30% $MgCl_2$ molten salt mixture but the oxide scale formed in this mixture spalled severely as seen in Figure 6(d). The oxide scale formed in 40% NaCl + 60% $CaCl_2$ molten salt mixture, which resulted in the lowest oxidation rate according to Figure 2, is more compact than other samples and has finer grain size as depicted in Figure 6(e).

Cross-sectional morphologies

Figure 7 shows morphologies of the cross-section of the corrosion products formed in four different single chloride molten salts after 20 h at 900°C. Distribution maps of

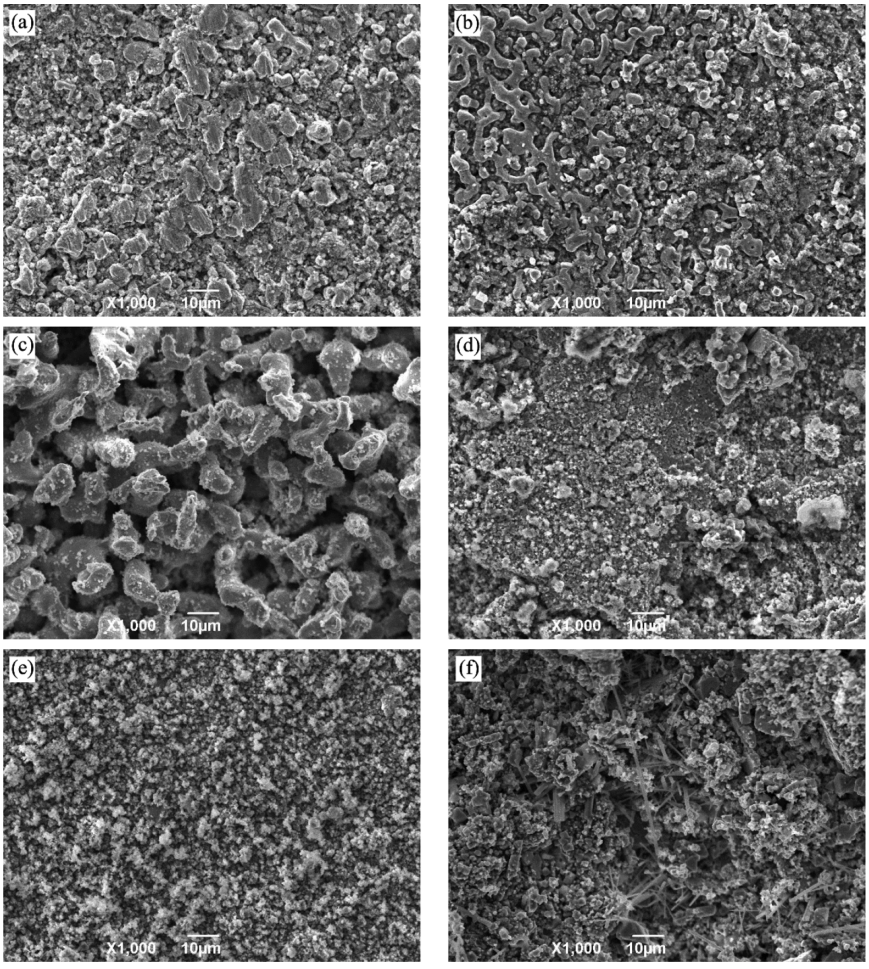

Figure 6: Surface morphologies of Inconel 625 after corrosion in (a) NaCl + $MgCl_2$ (2:3), (b) NaCl + $MgCl_2$ (7:3), (c) KCl + $MgCl_2$ (2:3), (d) KCl + $MgCl_2$ (7:3), (e) NaCl + $CaCl_2$ (2:3) and (d) KCl + $CaCl_2$ (2:3) mixture molten salts after 20 h at 900°C.

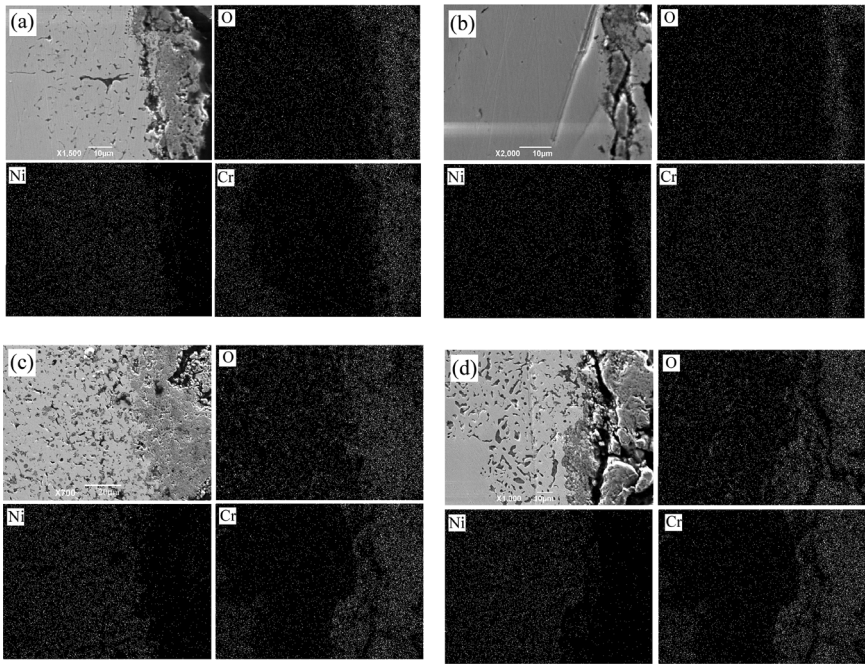

Figure 7: Cross-section views and elemental distribution maps of the corrosion products formed in (a) NaCl, (b) KCl, (c) $MgCl_2$ and (d) $CaCl_2$ molten salts after 20 h at 900°C.

O, Ni and Cr are also included. Three layers, bulk sample, inner corrosion layer, and oxide scale may be observed. Cracks were found in the oxide scales indicating that the oxide scales are non-protective and are prone to spallation. The inner corrosion layers formed in $MgCl_2$ and $CaCl_2$ molten salts are much thicker than those formed in NaCl and KCl molten salts. No obvious inner corrosion layer was found in the sample corroded in KCl molten salt. It can be seen from the distribution maps of the elements that the oxide scales are Cr enriched and Ni depleted while the inner corrosion layers are Cr depleted. The darker area in the inner corrosion layer was determined to be Cr_2O_3.

Cross-sections of the corrosion products formed in different mixtures of chloride molten salts after 10 h at 900°C are shown in Figure 8 along with distribution maps of the main elements. Corrosion time of 10 h was chosen to study morphologies of the early corrosion products. Similar to single salt corrosion, three layers are observed. Shorter oxidation time for these samples resulted in thinner oxide scale thickness. Corrosion penetrated deeper in $MgCl_2$-containing mixtures of molten salts than $CaCl_2$-containing mixtures; however, a more distinctive layer of oxide could be observed on the latter compared to the former. Also, the effect of KCl on corrosion was stronger than that of NaCl.

Discussion

Corrosion of Inconel 625 in chloride molten salts is different than in chloride-containing salts at temperature below melting point of the salts. In addition to the difference in the corrosion temperature, there is a difference in the oxygen partial pressure of the two corrosive environments. As an example, $MgCl_2$ does not react with Cr metal at temperature range of 400–600°C [6]; however, the present work observed that Inconel 625 underwent the most severe corrosion in $MgCl_2$ molten salts resulting in the formation of $MgCr_2O_4$, the reaction product of $MgCl_2$ and Cr as seen in Table 3. When the corrosion source is deposited as salt films the diffusion distance of oxygen is shorter and oxygen can be supplemented rapidly. Therefore, oxidation diffusion is the primary corrosion mechanism when the corrosion temperature is below the melting point of the salt film and chlorides accelerate the oxidation rate. In the present work, the samples were immersed in molten salts and oxygen partial pressure around the samples depended on the solubility and diffusion rate of oxygen in the molten salts. Thus, the corrosion mechanism of the metal alloy in the chloride molten salts cannot be explained simply by the "active oxidation" theory.

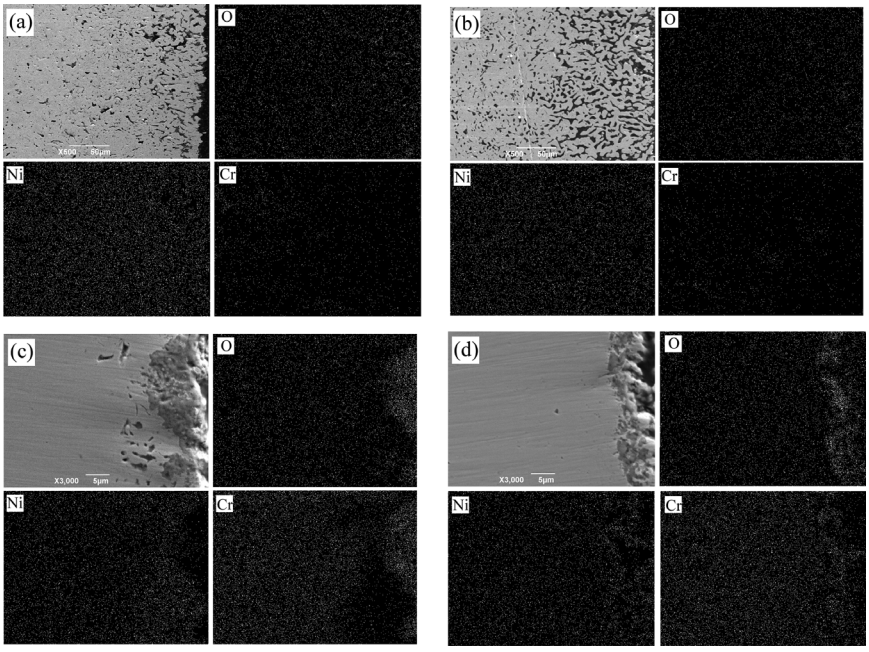

Figure 8: Cross-section views and elemental distribution maps of the corrosion products formed in (a) NaCl + $MgCl_2$ (2:3), (b) KCl + $MgCl_2$ (2:3), (c) NaCl + $CaCl_2$ (2:3) and (d) KCl + $CaCl_2$ (2:3) mixtures of molten salts after 20 h at 900°C.

The corrosion of metal alloys in the molten chloride salts should be different from those in the molten sulfate and carbonate salts because the molten chloride salts do not contain oxygen ions due to low oxygen solubility in chloride molten salt. It has been reported that the corrosion of Inconel 625 in the chloride molten salts is caused mainly by oxidant impurities in the molten salt [12]. During the present experiments, the oxygen ions in the molten salts should come from the reaction between the gases in the environment (mainly water vapor and oxygen) and the molten chloride salts.

$$4Cl^- + O_2 \rightarrow 2O^{2-} + 2Cl_2 \quad (1)$$

$$H_2O + 2Cl^- \rightarrow O^{2-} + 2HCl \quad (2)$$

The water vapor may come from the environment or from the hydrated chloride salt. Compared with alkali metal chloride, hydroscopicities of the alkaline earth metal chlorides are much higher. In fact, the alkali metal chloride (NaCl and KCl) used in the present work is anhydrous while the alkaline earth metal chloride ($CaCl_2$ and $MgCl_2$) is hydrous. Drying of the hydrous salts was not considered before the corrosion tests. The absorbed water and the water vapor in the environment will increase the basicity of the molten chloride salts through Reaction (2). In addition to the presence of water vapor, the vapor pressure of the molten chloride salt can also affect Reaction (1) since reaction between gases occurs more easily. The vapor pressure of the four chloride molten salts increases in the order of NaCl, KCl, $CaCl_2$ and $MgCl_2$. Vapor pressure of $MgCl_2$ is about two orders of magnitude higher than those of NaCl and KCl [13]. The exact basicity of the chloride molten salts at 900°C was not available in the present work; however, it is known that the basicity of alkaline earth metal molten chloride salts is higher than those of molten alkali metal chloride salts based on analysis of Reactions (1) and (2). Thus, it can be deduced that oxygen ion activity in the chloride molten salts increases in the order of NaCl, KCl, $CaCl_2$ and $MgCl_2$. As for the mixture chloride molten salts, the basicity depends on the constitutions and the mass ratios between the two chloride salts. The basicity of 40% NaCl + 60% $MgCl_2$ mixture should be higher than those of 40% NaCl + 60% $CaCl_2$ and 70% NaCl + 30% $MgCl_2$ mixtures.

At the initial stage of the corrosion in molten chloride salts, elements in the alloy, such as Ni and Cr, react with the oxygen dissolved in the molten salts to form NiO and Cr_2O_3 on the surface of the alloy. It has been known that [14] at low oxygen partial pressures oxidation of Cr takes precedence over Ni. Therefore, Cr_2O_3-enriched oxide scale will form on the surface of the alloy due to selective

oxidation of Cr. Solid reaction between NiO and Cr_2O_3 takes place to form $NiCr_2O_4$ spindle oxide as seen in Figures 3 and 4. As oxides form on the scale, they dissolve into the molten salts through the reactions:

$$2Cr_2O_3 + 4O^{2-} + 3O_2 \rightarrow 4CrO_4^{2-} \quad (3)$$

$$4NiO + 2O^{2-} + O_2 \rightarrow 4NiO_2^{-} \quad (4)$$

These ionic compounds diffuse into the molten salts, which explains the mass loss observed in the samples during corrosion tests in molten salt environments. Consequently, the oxide scales lose their protection against further corrosion. Based on the acidic-basicity dissolve model [15], the solubility of the oxide in the molten salts depends on the activity of oxygen ion (O^{2-}) in the molten salts. The higher the basicity of the molten salt, the easier dissolution of the oxide into the molten salt. This is in agreement with the corrosion rates presented in Figures 1 and 2.

However, as pointed out by some authors [10], it is surprising that the activity of oxygen ion in the chloride molten salts is lower than those in the sulfate and carbonate molten salts while the corrosion rate is much faster. The role of chlorine formed by Reaction (1) must be considered. Chlorine diffuses to the interface between oxide scale and metal alloy and reacts with Cr and Ni to form $CrCl_3$ and $NiCl_2$. Similar to oxide formation, $CrCl_3$ forms preferentially over $NiCl_2$. Owing to the high volatility of the metal chloride, chromium and nickel chlorides diffuse through the oxide scale to the sample surface. At the gas/molten salt interface, the metal chloride reacts with oxygen to form an oxide and freeing chlorine. This chlorine diffuses back to the oxide scale/metal alloy interface again. Oxidation of $CrCl_3$ occurs under lower oxygen partial pressure than $NiCl_2$. $CrCl_3$ can react with oxygen at the oxide scale and molten salts interface and deposit Cr_2O_3 on the oxide scale forming a porous and non-protective scale.

Volatilization and diffusion of $CrCl_3$ may create gas pressure high enough to damage the oxide scale and result in the formation of cracks and holes in the oxide scale. Consequently, chloride molten salts diffuse through the cracks and holes and make contact with the metal alloy, which accelerate the corrosion rate. The outer layer of the oxide scales is enriched in Cr as seen in Figures 7 and 8. The outer layer of the corrosion products formed in $CaCl_2$ and $MgCl_2$ single salt and the mixture salts melts peeled off during corrosion tests. Spallation of the corrosion products formed in NaCl and KCl salt melts was not observed. This is why the main compound shown in XRD of the corrosion products formed in $CaCl_2$ and $MgCl_2$ molten salts is $NiCr_2O_4$ as shown in Figures 3 and 4.

It is reported that NiO is more stable than Cr_2O_3 in chloride molten salts under neutral or basic conditions [10, 16]. The selective oxidation and chlorination of Cr in Inconel 625 cause depletion of Cr beneath the oxide scale. Because of the low oxygen and chlorine partial pressures and selective oxidation and chlorination along the grain boundaries of the alloy, these oxides cannot form a continuous layer and usually called “inner oxidation zone”.

The corrosion kinetics and the morphologies of the corrosion products are very different between the alkali metal chloride and alkaline earth metal chloride molten salts. Cations in the molten chloride salt seem to affect the thermal and chemical properties of the salt such as vapor pressure and hydroscopicities, which can affect the basicity of the molten salt. In the present work, no evidence was observed indicating that cations react with Cr to form alkali or alkaline earth metal chromates except $MgCl_2$, which has been considered by some investigations to be one of the reasons causing the damage to the oxide scale [5]. However, this possibility cannot be eliminated because of low sensitivity of XRD analysis.

Conclusions

Corrosion of Inconel 625 in four chloride molten salts and their mixtures was studied with an emphasis on the effects of cations in chloride molten salts. Because of higher vapor pressures and hydroscopicities of the alkaline metal chloride molten salts, which result in the higher basicity of the molten salts, Inconel 625 corrosion suffers server corrosion in $CaCl_2$ and $MgCl_2$ molten salts and mixture molten salts with high $CaCl_2$ and $MgCl_2$ contents. Except for $MgCl_2$, no evidence for reaction of cations with Cr to form alkali or alkaline earth metal chromates was observed. Cations in the molten chloride salt seem to affect the thermal and chemical properties of the salt.

Funding: This work was financially supported by National Science Foundation of China (NSFC) under the grant nos. 51201131 and Science and Technology Program of Shaanxi Province, China (2013KJXX-42). It was also supported by the National Science Foundation (NSF) CREST Grant HRD-0932421.

References

[1] H.P. Nielsen, F.J. Frandsen, K. Dam-Johansen and L.L. Baxter, Prog. Energy Combust. Sci., 26 (2000) 283–298.
[2] B.P. Mohanty and D.A. Shores, Corros. Sci., 46 (2004) 2893–2907.
[3] D.A. Shores and B.P. Mohanty, Corros. Sci., 46 (2004) 2909–2924.
[4] J.E. Indacochea, J.L. Smith, K.R. Litko, E.J. Karell and A.G. Raraz, Oxid. Met., 55 (2001) 1–16.
[5] H.J. Grabke, E. Reese and M Spiegel, Corros. Sci., 37 (1995) 1023–1043.
[6] J. Lehmusto, B.J. Skrifvars, P. Yrjas, and M. Hupa, Corros. Sci., 53 (2011) 3315–3323.
[7] J. Pettersson, H. Asteman, J.-E. Svensson and L.-G. Johansson, Oxid. Met., 64 (2005) 23–41.
[8] S. Enestam, D. Bankiewicz, J. Tuiremo, K. Mäkelä and M. Hupa, Fuel, 104 (2013) 294–306.
[9] P. Viklund, A. Hjörnhede, P. Henderson, A. Stälenhein and R. Pettersson, Fuel Process. Technol., 105 (2013) 106–112.
[10] T. Ishitsuka and K. Nose, Materials and Corrosion, 51 (2000) 177–181.
[11] Y. Kawahara, Corros. Sci., 44 (2002) 223–245.
[12] F. Colom and A. Bodalo, Corros. Sci., 12 (1972) 731–734.
[13] G.J. Janz, R.P.T. Tomkins, J.R. Downey, G.L. Gardner, U. Krebs and S.K. Singer, J Phys. Chem. Ref. Data, 4 (1975) 871–1178.
[14] N. Birks, G.H. Meier and F. Pettit, Introduction to the High Temperature Oxidation of Metals, Cambridge University Press, Cambridge (2006).
[15] R.A. Rapp, Corros. Sci., 44 (2002) 209–221.
[16] T. Ishitsuka and K. Nose, Corros. Sci., 44 (2002) 247–263.